STATISTICALLY OPTIMISED NEAR FIELD ACOUSTIC HOLOGRAPHY BASED ON PARTICLE VELOCITY MEASUREMENTS

Finn Jacobsen* and Virginie Jaud

Acoustic Technology, Ørsted•DTU, Technical University of Denmark, Building 352, Ørsteds Plads, DK-2800 Kgs. Lyngby, Denmark
fja@oersted.dtu.dk

Abstract

Statistically optimised near field acoustic holography (SONAH) is a variant of conventional near field acoustic holography (NAH) that avoids spatial Fourier transforms and thus some of the errors and limitations caused by spatial transforms. In particular the spectral leakage caused by the spatial windows in the NAH procedure is avoided, and thus the usual requirement of a measurement aperture that extends well beyond the source can be relaxed. Both NAH and SONAH are usually based on measurement of the sound pressure. However, a recent investigation has showed that NAH based on measurement of the acoustic particle velocity is more accurate and less sensitive to transducer mismatch errors that NAH based on measurement of the sound pressure. In this investigation it is examined whether there is a similar advantage in using the particle velocity in SONAH.

INTRODUCTION

Near field acoustic holography (often abbreviated NAH) is an experimental technique that makes it possible to reconstruct three-dimensional sound fields from measurements on two-dimensional surfaces. This can be extremely useful, and NAH is a well-established tool for visualising and analysing sound fields near sources of noise.[1,2] Conventional NAH is based on discrete spatial Fourier transforms of sound pressure data measured with a microphone array. However, to reduce truncation errors caused by the spatial transform (‘leakage’ in the wavenumber domain) the array must extend beyond the source so that the sound pressure has dropped to an insignificant level near the edges of the array.[2]

Statistically optimised near field acoustic holography (SONAH) is an interesting variant of NAH developed by Steiner and Hald.[3] It has the great advantage of

Eds.: J. Eberhardsteiner, H.A. Mang, H. Waubke

avoiding spatial transforms and thus the mentioned truncation effects; therefore the measurement array can be smaller than the source.[3-6] Both NAH and SONAH are usually based on measurement of the sound pressure. However, an acoustic particle velocity transducer is now available,[7] and it has recently been demonstrated that NAH based on measurement of the normal component of the particle velocity is more accurate than pressure-based NAH.[8] Thus the purpose of this paper is to examine whether there is a similar advantage in using the particle velocity with the SONAH procedure.

OUTLINE OF THEORY

The following brief derivation essentially follows Hald.[4,5] In planar SONAH the 'propagator' that transforms data from one plane to another is not a multiplication in the wavenumber domain as in NAH,[1,2] but a transfer matrix that works directly on the measured data, that is, the sound pressure at an arbitrary position above the source, $\mathbf{r} = (x, y, z)$ (where $z > 0$), can be expressed as a weighted sum of sound pressures measured at N positions ($\mathbf{r}_{h,n}$) in the hologram plane ($z = z_h$),

$$p(\mathbf{r}) \simeq \sum_{n=1}^{N} c_n(\mathbf{r})\, p(\mathbf{r}_{h,n}) = \mathbf{p}^{\mathrm{T}}(\mathbf{r}_h)\mathbf{c}(\mathbf{r}), \tag{1}$$

where $^{\mathrm{T}}$ indicate that the column vector $\mathbf{p}(\mathbf{r}_h)$ is transposed. The transfer vector $\mathbf{c}(\mathbf{r})$ does not depend on the sound field but only on positions. It is determined by requiring that an infinite set of propagating and evanescent elementary waves,

$$\Phi_m(\mathbf{r}) = \mathrm{e}^{-\mathrm{j}(k_{x,m}x + k_{y,m}y + k_{z,m}z)}, \quad m = 1, 2, \ldots M,\ M \to \infty, \tag{2}$$

where

$$k_{z,m} = \begin{cases} \sqrt{k^2 - k_{x,m}^2 - k_{y,m}^2} & \text{for } k \geq \sqrt{k_{x,m}^2 + k_{y,m}^2}, \\ -\mathrm{j}\sqrt{k_{x,m}^2 + k_{y,m}^2 - k^2} & \text{for } k < \sqrt{k_{x,m}^2 + k_{y,m}^2}, \end{cases} \tag{3}$$

are projected from the measurement plane to the prediction plane (in other words, satisfy eq. (1)) with optimal accuracy. Thus, in vector and matrix form,

$$\boldsymbol{\alpha}(\mathbf{r}) \simeq \mathbf{A}\mathbf{c}(\mathbf{r}), \tag{4}$$

where $\boldsymbol{\alpha}(\mathbf{r})$ is a column vector with M elements, $\left[\boldsymbol{\alpha}(\mathbf{r})\right]_m = \Phi_m(\mathbf{r})$, and $\mathbf{A}$ is an M by N matrix, $\left[\mathbf{A}\right]_{mn} = \Phi_m(\mathbf{r}_{h,n})$. Since $M > N$ eq. (4) is overdetermined and can be solved for $\mathrm{c}(\mathbf{r})$ only in the least squares sense. The result is[3-5]

$$\mathbf{c}(\mathbf{r}) = \left(\mathbf{A}^{\mathrm{H}}\mathbf{A} + \theta^2\mathbf{I}\right)^{-1} \mathbf{A}^{\mathrm{H}}\boldsymbol{\alpha}(\mathbf{r}), \tag{5}$$

where $\mathbf{I}$ is the identity matrix, θ is a regularisation parameter, and $^{\mathrm{H}}$ indicate the Hermitian transpose. Note that $\mathbf{A}^{\mathrm{H}}\mathbf{A}$ is an N by N matrix and $\mathbf{A}^{\mathrm{H}}\boldsymbol{\alpha}(\mathbf{r})$ is a column vector with N elements. It now follows that the sound pressure in the prediction plane is

$$p(\mathbf{r}) = \mathbf{p}^{\mathrm{T}}(\mathbf{r}_h)\left(\mathbf{A}^{\mathrm{H}}\mathbf{A} + \theta^2\mathbf{I}\right)^{-1}\mathbf{A}^{\mathrm{H}}\boldsymbol{\alpha}(\mathbf{r}). \quad (6)$$

The normal component of the particle velocity in the prediction plane is obtained from eq. (6) using Euler's equation of motion,

$$u_z(\mathbf{r}) = \frac{-1}{\mathrm{j}\omega\rho}\mathbf{p}^{\mathrm{T}}(\mathbf{r}_h)\left(\mathbf{A}^{\mathrm{H}}\mathbf{A} + \theta^2\mathbf{I}\right)^{-1}\frac{\partial\mathbf{A}^{\mathrm{H}}\boldsymbol{\alpha}(\mathbf{r})}{\partial z} = \mathbf{p}^{\mathrm{T}}(\mathbf{r}_h)\left(\mathbf{A}^{\mathrm{H}}\mathbf{A} + \theta^2\mathbf{I}\right)^{-1}\mathbf{A}^{\mathrm{H}}\boldsymbol{\beta}(\mathbf{r}), \quad (7)$$

where the only quantity that is differentiated is the vector $\mathbf{A}^{\mathrm{H}}\boldsymbol{\alpha}(\mathbf{r})$ since this is the only quantity that depends on z. Inspection of eq. (4) leads to the conclusion that the transfer vector given by eq. (5) also projects the normal component of the particle velocity from the measurement plane to the prediction plane,

$$u_z(\mathbf{r}) = \mathbf{u}_z^{\mathrm{T}}(\mathbf{r}_h)\left(\mathbf{A}^{\mathrm{H}}\mathbf{A} + \theta^2\mathbf{I}\right)^{-1}\mathbf{A}^{\mathrm{H}}\boldsymbol{\alpha}(\mathbf{r}). \quad (8)$$

Finally, the sound pressure in the prediction plane can be calculated from eq. (8),

$$p(\mathbf{r}) = \mathbf{u}_z^{\mathrm{T}}(\mathbf{r}_h)\left(\mathbf{A}^{\mathrm{H}}\mathbf{A} + \theta^2\mathbf{I}\right)^{-1}(-\mathrm{j}\omega\rho)\int\mathbf{A}^{\mathrm{H}}\boldsymbol{\alpha}(\mathbf{r})\mathrm{d}z = \mathbf{u}_z^{\mathrm{T}}(\mathbf{r}_h)\left(\mathbf{A}^{\mathrm{H}}\mathbf{A} + \theta^2\mathbf{I}\right)^{-1}\mathbf{A}^{\mathrm{H}}\boldsymbol{\gamma}(\mathbf{r}), \quad (9)$$

where the only quantity that is integrated is the vector $\mathbf{A}^{\mathrm{H}}\boldsymbol{\alpha}(\mathbf{r})$ since this is the only quantity that depends on z.

In practice it is usually desirable to estimate pressures and particle velocities not just at a single position $\mathbf{r}$ but at a grid of N points in a plane; thus the column vectors $\mathbf{A}^{\mathrm{H}}\boldsymbol{\alpha}$, $\mathbf{A}^{\mathrm{H}}\boldsymbol{\beta}$ and $\mathbf{A}^{\mathrm{H}}\boldsymbol{\gamma}$ become N by N matrices, and the left-hand sides of eqs. (6), (7), (8) and (9) become column vectors. In the limit of $M \to \infty$ the elements of $\mathbf{A}^{\mathrm{H}}\mathbf{A}$, $\mathbf{A}^{\mathrm{H}}\boldsymbol{\alpha}$, $\mathbf{A}^{\mathrm{H}}\boldsymbol{\beta}$ and $\mathbf{A}^{\mathrm{H}}\boldsymbol{\gamma}$ turn into integrals over k_x and k_y that can be evaluated numerically.[3-5]

To summarise, the SONAH procedure makes it possible to predict the sound pressure and the particle velocity from measured sound pressures using eqs. (6) and (7), and to predict the particle velocity and the sound pressure from measured particle velocities using eqs. (8) and (9).

A SIMULATION STUDY

The performance of the measurement procedure described above has been examined in a simulation study. The first test case was a vibrating steel panel with a thickness of 5 mm and dimensions 21 by 21 cm mounted simply supported in an infinite baffle and driven by a point force of 10 N near a corner. This was modelled by a conventional modal sum. In what follows this configuration is referred to as the 'small panel'. The second test case consisted of two plane waves propagating in the yz-plane at angles of $\pm 40^\circ$ from the normal to the z-plane. Such interfering plane waves travelling in oblique directions might conceivably be generated by a standing bending wave in an infinite plate at $z = 0$ (or two interfering bending waves travelling in opposite directions) with a bending wavelength that is 55% larger than the speed of sound. The last test case was a baffled panel with dimensions 1 by 1 m and identical to the small

panel except for its size. In all cases the measurement plane was 6 cm from the source, the prediction plane was 3 cm from the source, and both the measurement plane and the prediction plane had dimensions 21 by 21 cm. There were 8 by 8 transducers in the measurement array, corresponding to a distance of 3 cm between adjacent transducers, the prediction points were placed in a similar grid, and the centres of the measurement plane, the prediction plane, and both panels were placed at $(x, y) = (0, 0)$. The value of the regularisation parameter θ corresponded to a signal-to-noise ratio of 40 dB.[3-5] The sound pressure and the z-component of the particle velocity generated by the two panels at the 64 transducer positions were calculated using a numerical approximation to Rayleigh's first integral,[2] and the 'true' values of the sound pressure and the z-component of the particle velocity in the prediction plane were calculated in the same manner.

Ideal Transducers

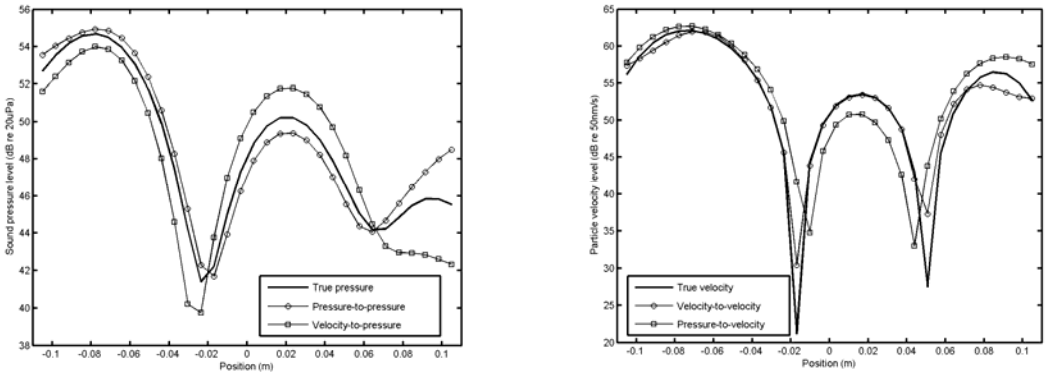

Figure 1 – Small panel driven at 500 Hz. The left-hand figure shows the 'true' and predicted sound pressure, and the right-hand figure shows the 'true' and predicted particle velocity.

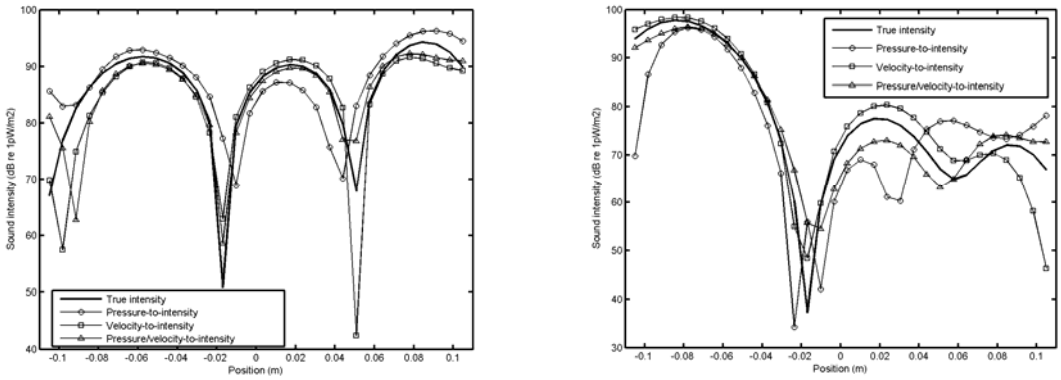

Figure 2 – 'True' and predicted sound intensity near the small panel driven at 500 Hz (left figure) and at 1 kHz (right figure).

Figures 1 and 2 show the results of the simulated measurements near the small panel. Both figures compare SONAH predictions with the corresponding 'true' values in a line across the prediction plane. It is apparent from fig. 1 that the prediction of the pressure based on pressure measurements is slightly better than the corresponding

prediction based on particle velocity data; and it can also be seen that the prediction of the velocity based on velocity data is better than the corresponding prediction based on pressure data. Note that the particle velocity level is shown relative to 50 nm/s.

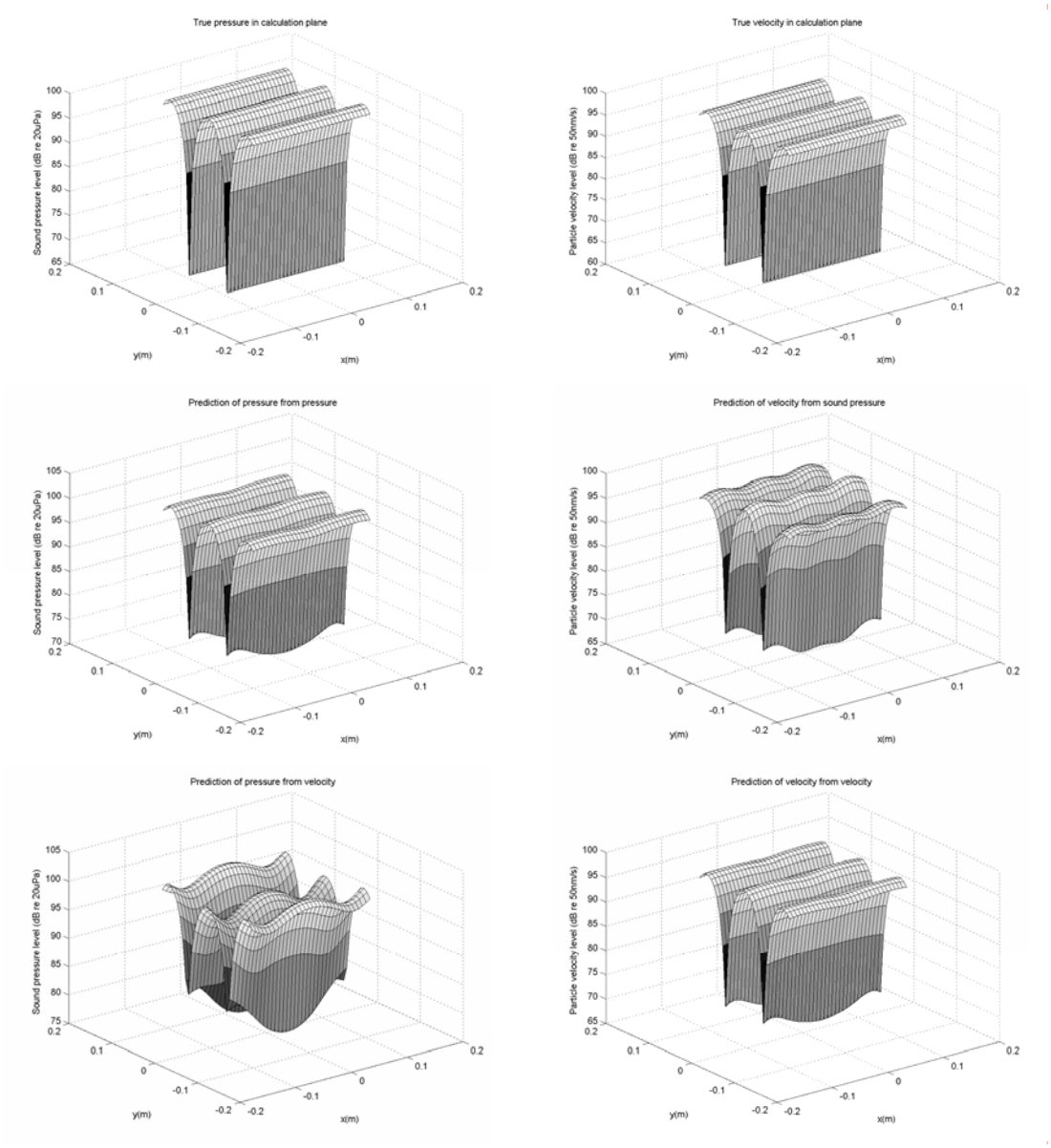

Figure 3 – Two interfering plane wave generated by a standing bending wave in an infinite plane vibrating at 3 kHz. Top left, true pressure; top right, true particle velocity; middle left, pressure from pressure; middle right, velocity from pressure; bottom left, pressure from velocity; bottom right, velocity from velocity.

Inspection of fig. 2 leads to the conclusion that the best prediction of the sound intensity is obtained if it is based on both pressure and velocity data; the prediction is slightly less accurate if it is based solely on particle velocity data, and the prediction

based on pressure data is the least accurate. In other words, it seems advantageous to measure both sound pressure and particle velocity. Note that the measurement and prediction planes have the same size as the source, confirming that SONAH does not require measurement arrays larger than the source.

The test case with two interfering plane waves serves the purpose of subjecting the SONAH procedure to a source that is infinitely larger than the array. It is also an extreme case in the sense that it corresponds to two delta functions in the wavenumber domain; in other words, it is extremely far from the 'white noise' in the source plane inherently assumed in the optimisation used in solving eq. (4).[3,4] The results, shown in fig. 3, confirm that SONAH can indeed cope with large sources. The observations from fig. 1 are also confirmed, that is, pressure-to-pressure is better that particle velocity-to-pressure, and particle velocity-to-particle velocity is better than pressure-to-particle velocity.

The Influence of Transducer Mismatch

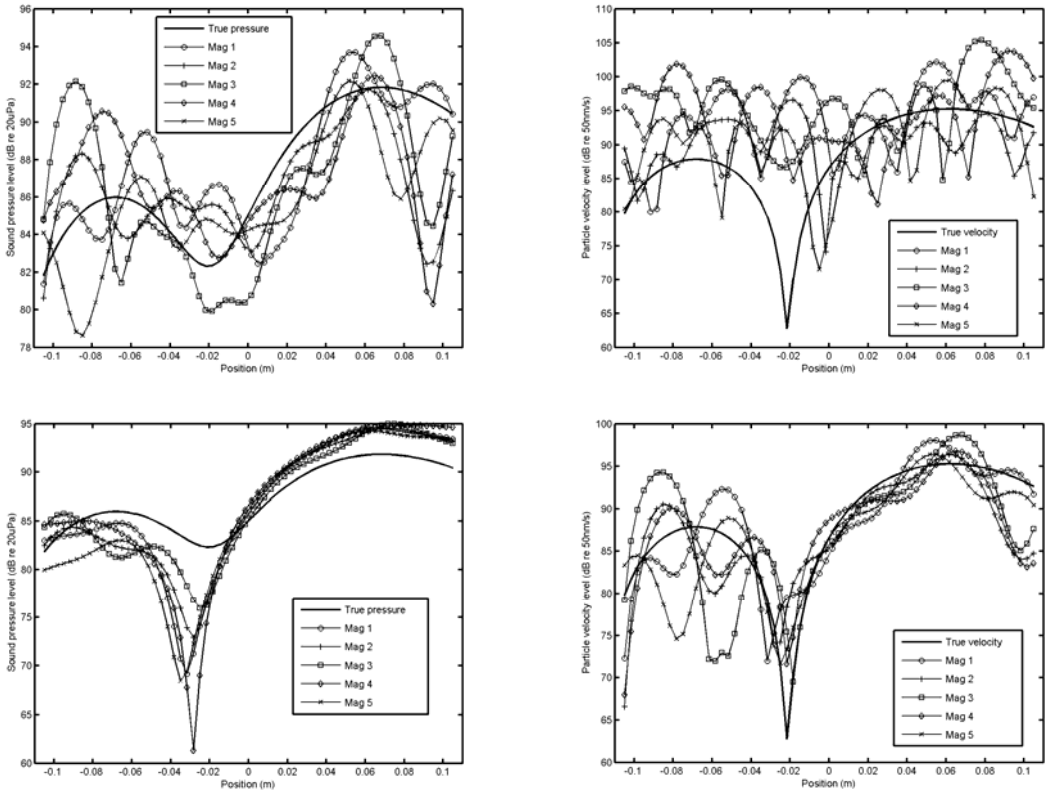

Figure 4 – The influence of transducer amplitude mismatch on predictions near the large panel driven at 500 Hz. Top left, pressure predicted from pressure; bottom left, pressure predicted from particle velocity; top right, particle velocity predicted from pressure; bottom right, particle velocity predicted from particle velocity.

The last test case was the large panel. In the predictions shown in fig. 4 random transducer amplitude mismatch evenly distributed between ±0.5 dB has been introduced;

the figure shows five outcomes of this stochastic experiment. It is apparent that such amplitude mismatch has a serious influence on the performance of the SONAH procedure. By far the most serious influence occurs when the particle velocity is predicted from pressure data. The results shown in fig. 5 have been calculated by introducing random phase mismatch evenly distributed between $\pm 2^{\circ}$. A clear degradation of the accuracy can be seen, although this amount of phase mismatch is less serious that amplitude mismatch of ± 0.5 dB. Again the most serious influence occurs in predictions of the particle velocity from pressure data. Predictions of the particle velocity from particle velocity data are the least affected.

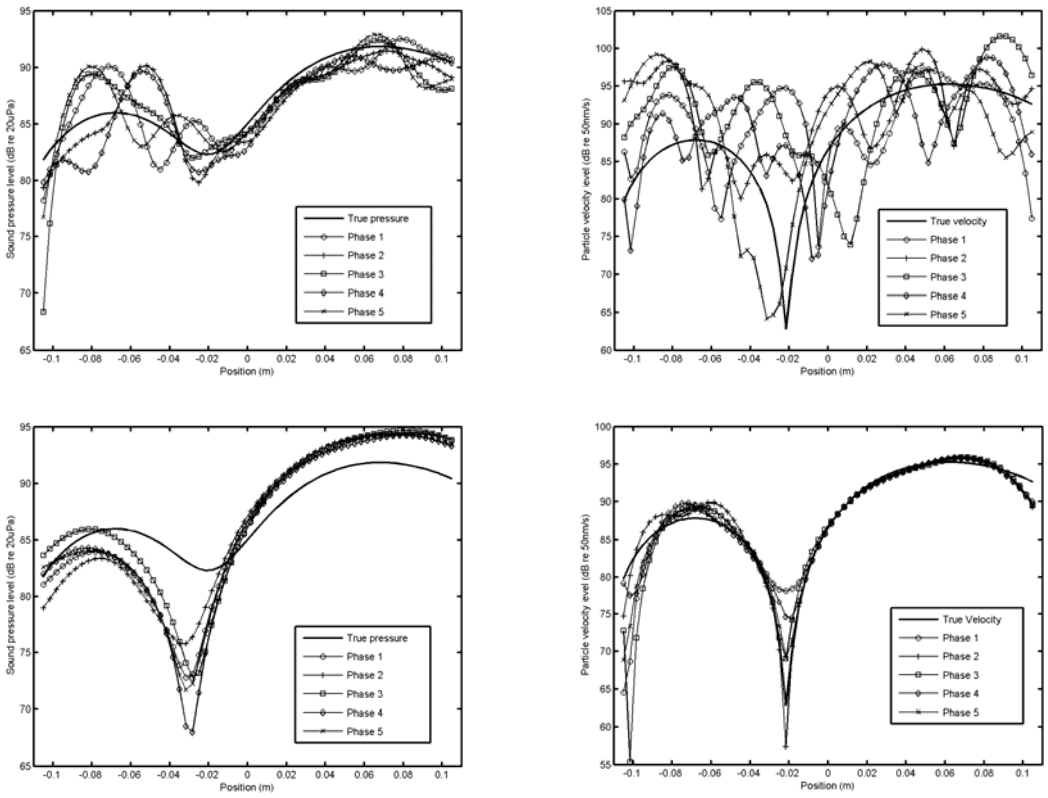

Figure 5 – The influence of phase mismatch on predictions near the large panel driven at 500 Hz. Top left, pressure predicted from pressure; bottom left, pressure predicted from particle velocity; top right, particle velocity predicted from pressure; bottom right, particle velocity predicted from particle velocity.

DISCUSSION

A recent investigation of conventional NAH concluded that the accuracy of pressure-to-pressure predictions is comparable to the accuracy velocity-to-velocity predictions, whereas the accuracy of velocity-to-pressure predictions is far better than the accuracy of pressure-to-velocity predictions.[8] It was also concluded that transducer mismatch has a significantly more serious influence on pressure-to-velocity predictions

than on velocity-to-pressure predictions. In both cases the explanation was that the wavenumber ratio that occurs in the propagator when the pressure is predicted from the particle velocity reduces high spatial frequencies, whereas the wavenumber ratio that occurs when the particle velocity is predicted from the pressure amplifies them.[8]

The tendencies observed with SONAH predictions are similar, but less extreme; on the whole velocity-to-pressure predictions are better than pressure-to-velocity predictions, in particular if the transducers are not perfectly matched. Presumably the explanation is the same as with NAH; although transforms to the wavenumber domain are avoided, high spatial frequencies are nevertheless reduced in the former case and amplified in the latter case. An additional advantage of particle velocity-based conventional NAH is that the normal component of the particle velocity because of the necessary, large measurement plane decreases faster towards the edges of the plane than the pressure does, which reduces spatial windowing effects.[8] This effect is not important with the SONAH procedure.

It should finally be mentioned that the same regularisation have been used in all test cases, but more regularisation would undoubtedly improve the SONAH performance in case of transducer mismatch.

CONCLUSIONS

A simulation study has confirmed that statistically optimised near field acoustic holography (SONAH) can cope with sources larger than the measurement array, and demonstrated that SONAH based on measurement of the particle velocity is somewhat more accurate than SONAH based on pressure measurements, in particular if the transducers are not matched very well. In predicting sound intensity the best results are obtained if both pressure and velocity signals are measured.

REFERENCES

1 J.D. Maynard, E.G. Williams and Y. Lee, 'Nearfield acoustic holography. I. Theory of generalized holography and the development of NAH,' *J. Acoust. Soc. Am.* **78**, 1395-1413 (1985)

2 E.G. Williams, *Fourier Acoustics—Sound Radiation and Nearfield Acoustical Holography* (Academic Press, San Diego, 1999)

3 R. Steiner and J. Hald, 'Near-field acoustical holography without the errors and limitations caused by the use of spatial DFT', *Int. J. Acoust. Vib.* **6**, 83-89 (2001)

4 J. Hald, 'Planar near-field acoustical holography with arrays smaller than the sound source,' *Proc. 17th International Congress on Acoustics*, Vol. 1, pp. 168-169, Rome, Italy, 2001

5 J. Hald, 'Patch near-field acoustical holography using a new statistically optimal method,' Proceedings of Inter-Noise 2003, pp. 2203-2210, Jeju Island, Korea, 2003

6 Y.T. Cho, J. Stuart Bolton and J. Hald, 'Source visualization by using statistically optimized near-field acoustical holography in cylindrical coordinates,' *J. Acoust. Soc. Am.* **118**, 2355-2364 (2005)

7 R. Raangs, W.F. Druyvesteyn and H.-E. de Bree, 'A low-cost intensity pro*be,' J. Audio Eng. Soc.* **51**, 344-357 (2003)

8 F. Jacobsen and Y. Liu, 'Near field acoustic holography with particle velocity transducers,' *J. Acoust. Soc. Am.* **118**, 3139-3144 (2005)